Compact UWB Pi-Slotted Elliptical Patch Antenna for Terahertz Applications

Md. Sulaiman and Abu Zafor Md. Touhidul Islam

***Abstract*—Antennas offering wide bandwidth, high gain and efficiency are essential to terahertz (THz) wireless communication systems and has gathered significant attention in antenna research. This paper introduces a compact, high-gain, ultra-wideband (UWB) microstrip patch antenna tailored for THz applications, along with its performance analysis. The proposed antenna has an elliptical patch with a pi shaped slot and is excited by a tapered feedline. An elliptical patch antenna incorporating a pi-shaped slot is introduced for the first time in the terahertz THz spectral region, demonstrating the ability to simultaneously achieve substantial size miniaturization, wideband performance, improved impedance matching, and enhanced gain. The antenna structure was designed and optimized for improved performance using CST Microwave Studio (MWS) version 2018. A Rogers RT/duroid 5880 substrate was used for antenna design, featuring 6 µm thickness, 2.2 relative permittivity, 0.0009 loss tangent, and 120 × 80 µm² planar dimensions. The proposed antenna demonstrates strong performance characteristics with a wide impedance bandwidth of 3.41 THz (5.01–8.42 THz), high gain of 7.906 dB, radiation efficiency of 77.83%, and low return loss of −43.57 dB, with consistent VSWR across the entire frequency range. The surface current distribution as well as the input impedance of the pi-shaped slotted antenna are also favorable. All the simulation results suggest that the proposed small size pi-shaped slotted elliptical patch antenna can be a suitable candidate for high-speed 6G wireless communication applications in the THz band.**

***Index Terms*—Elliptical patch, microstrip antenna, pi shaped slot, tapered feedline, terahertz band, wideband, wireless applications, 6G communication.**

Original Research Paper
DOI: 10.53314/ELS2630029S

I. Introduction

OVER the past few decades, bandwidth requirements for wireless communications have increased rapidly. Although advanced modulation techniques have been employed to enhance spectral efficiency [1], the channel capacity is ultimately limited by Shannon's formula, even with MIMO implementations. Consequently, accessing higher carrier frequency bands like terahertz (THz) spectrum (0.1 to 10 THz) is essential to meet the required transmission capacity. Owing to the unique advantages like broadband capability, secure, more directional, smaller scintillation effects, low attenuation, and low energy consumption, THz technology has been applied in the field of communication, defense, biomedical imaging, spectroscopy, and radio astronomy [2], [3]. Research in THz technology has grown recently, driven by the availability of THz sources and progress in laser, semiconductor, and photoconductive technologies [4]. THz antenna design suffers from severe signal attenuation, fabrication challenges associated with microscopic dimensions, and significant material losses. Antennas functioning within the THz band must demonstrate high gain, wide bandwidth, high directive and minimal signal losses to ensure robust and efficient communication [5], [6].

Patch antennas have attracted considerable attention as a promising solution for THz applications owing to their compact dimensions, ease of fabrication, and compatibility with integrated circuit technology. A dual-band reconfigurable graphene-based antenna detailed in [7] achieved a bandwidth of 50 GHz with a gain of 4.01 dB. Photonic band gaps and defective ground structures were utilized in [8], which leads to a gain increase to 6.93 dB. But it suffers from narrow bandwidth and size limitations. A miniaturized graphene-based THz patch antenna proposed in [9] obtained a high return loss of −57.54 dB and a bandwidth of 199.6 GHz, though its gain was limited to 2.76 dB. An asymmetric coplanar waveguide-fed patch antenna was developed in [10], which offered a gain of 6.14 dB and a compact design but with a narrower bandwidth of 92 GHz. Moulfi et al. developed a wideband nano circular graphene-printed antenna for terahertz transmission, employing a Defected Ground Structure (DGS) technique to enhance bandwidth and conducted a parametric study [11]. Khan et al. proposed a circular THz patch antenna and investigated variations in substrate shapes and materials [12]. Abohmra et al. examined the characteristics of graphene at terahertz frequencies through a rectangular antenna designed for wearable applications [13]. Fakharian introduced a multifunctional graphene-based THz antenna [14], while Badr and Moradi presented a novel hexagonal dual-band antenna operating at 2.14 THz and 5.41 THz [15]. Nissiyah and Madhan explored graphene-based patch antennas capable of supporting triple and quad-band operations in the terahertz range [16].

Manuscript received on November 7th, 2025. Received in revised form on February 18th and March 18th, 2026. Accepted for publication on March 30th, 2026.

Sulaiman is with the Antenna Design Lab, Department of Electrical and Electronic Engineering, University of Rajshahi, Rajshahi 6205, Bangladesh (e-mail: mdsulaiman113504@gmail.com, ORCiD: 0009-0009-7451-8842).

Abu Zafor Md. Touhidul Islam is with the Antenna Design Lab, Department of Electrical and Electronic Engineering, University of Rajshahi, Rajshahi 6205, Bangladesh (e-mail: touhid.eee@ru.ac.bd, ORCiD: 0009-0002-0375-4660).

Although numerous THz antennas have been proposed, most suffer from either large physical dimensions or limitations in bandwidth, gain, and efficiency. These shortcomings pose significant challenges for practical THz system implementation [17]. Thus, further investigation into patch antenna structures is essential to achieve improved performance. This study presents the design and performance analysis of a compact, high-performance pi-slotted elliptical patch antenna tailored for THz-band 6G communication systems. Elliptical geometries provide efficient current distribution, reduced surface-wave losses, minimized cross-polarization levels, broader impedance bandwidth, and the potential for enhanced gain and directivity [18]. Incorporating slots into the design can further improve impedance matching and radiation efficiency, which are critical for effective 6G communication [17], [19]. A pi-shaped slotted microstrip patch antenna is considered superior for modern wireless communication due to its ability to enhance performance metrics simultaneously, such as achieving wide impedance bandwidth, high gain, high efficiency, and compact size. The pi-slot geometry acts as a reactive loading technique that alters the surface current distribution, improving impedance matching and enabling multi-frequency operation. The novelty of employing a pi-shaped slot in elliptical patch antenna design lies in its first introduction within the THz spectral region, where it demonstrates the capacity to simultaneously achieve substantial size miniaturization, wideband or multi-band performance, improved impedance matching, and gain.

The rest of the paper is arranged as follows. The antenna design approach is discussed in Section II. Section III presents the simulation results and performance analysis of the proposed antenna. A comparison of the proposed antenna's performance with previously reported designs is given in Section IV. Finally, key findings of the research are listed in Section V.

II. Proposed Antenna Design

The proposed antenna has been designed and simulated using CST Studio Suite 2018. An elliptical patch with a pi-slot, a full ground, and a 50 Ω feedline are incorporated in the proposed pi-shaped slotted elliptical patch antenna. The feedline is tapered from a wider base to a narrower tip used for better impedance matching. Fig. 1 shows the front-facing view and pi-slot structure of the proposed THz antenna. The substrate material used is Rogers RT/duroid 5880, with a relative permittivity (εr) of 2.2 a loss tangent (tan δ) of 0.0009. A substrate of 6 μm thickness is used, and the patch, full ground, and feedline structure are fabricated from annealed copper with a thickness of 0.035 mm. This design methodology reflects a hybrid approach combining: Geometric shaping of radiating Element (elliptical patch) for smooth current distribution and broad radiation characteristics, Slot loading (Pi-shaped slot) enables multi-resonance tuning, broader bandwidth and higher radiation efficiency, Parametric control for fine-tuning of performance metrics.

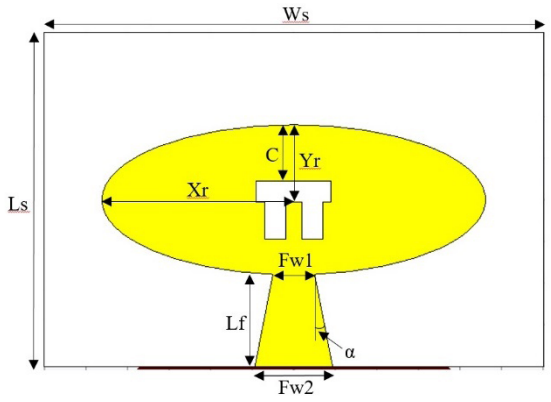

(a)

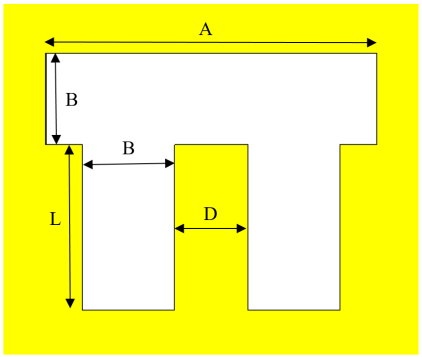

(b)

Fig. 1. (a) Front-facing view and (b) Pi-shaped slotted elliptical patch antenna.

The subsequent phase in the design process involves establishing the dimensions of the antenna structure, which are directly affected by its resonant frequency. This antenna is intended to function within a frequency range of 4.5-9.5 THz, with an operational frequency set at 5.5 THz. At this frequency, the wavelength of the signal is considerably shorter than that at lower frequencies, significantly influencing the antenna's dimensions. When designing an elliptical patch antenna, it is essential to determine both the semi-major axis and semi-minor axis of the patch. This calculation relies on the targeted resonant frequency, substrate properties, and operating environment conditions.

The semi-major axis of the elliptical patch is computed as follows [20], [21],

$$a \approx \frac{\lambda_d}{2} \tag{1}$$

where λ_d is the wavelength in the dielectric medium which can be calculated as

$$\lambda_d = \frac{c}{f_0 \sqrt{\varepsilon_{reff}}} \tag{2}$$

where ε_{reff} is the substrate's effective dielectric constant,

$$\varepsilon_{reff} = \frac{\varepsilon_r + 1}{2} + \frac{\varepsilon_r - 1}{2}\left(1 + \frac{12h}{w}\right)^{-1/2} \quad (3)$$

Here, ε_r the relative permittivity, w the width and h the height of the substrate, c the speed of light, and f_0 being the resonant frequency of the antenna. And semi-minor axis, b of an elliptical patch is calculated as

$$b = \frac{a}{AR} \quad (4)$$

where, AR is the aspect ratio, which is chosen based on the design requirements and radiation characteristics.

The optimize design parameters of the proposed THz antenna are presented in Table I. Key design parameters, including substrate dimensions, elliptical patch axes, feedline tapering, and Pi-slot geometry, are carefully tuned to support dual-band THz operation. The compact size of the designed antenna is 120 µm × 80 µm^2. The pi-shaped slotted elliptical antenna is excited using a 50 Ω tapered feedline, with the impedance maintained at 50 Ω to achieve high performance.

TABLE I
OPTIMAL VALUES OF DESIGN PARAMETERS

Parameters (symbol)	Value (µm)
Width of substrate (Ws)	120
Length of substrate (Ls)	80
Thickness of substrate	6
Semi major axis (Xr)	46
Semi minor axis (Yr)	17.96
Thickness of patch & ground	1.2
Length of feedline (Lf)	22.04
Top-end width of feedline (Fw1)	8
Bottom-end width of feedline (Fw2)	18.64
Taper angle (α)	11.07º
Pi slot length (A)	18
Width of pi slot (B)	5
Legs length of pi slot (L)	9
Distance between the legs of pi slot (D)	4
Top-to-slot offset (C)	13.46

Tuning the pi-slot geometry is achieved through systematic parametric variation in CST. CST allows defining the pi-slot length, width, and position as parameters. These are varied systematically to observe their effect on S11 (return loss). Authors run multiple simulations, adjusting geometry until the desired THz band performance is achieved.

The shape of the initially designed radiating element is an elliptical patch. The original elliptical patch is modified by inserting a pi-shaped slot. A pi-shaped slot can create multiple current paths, enabling broadband operation. This slot is etched for impedance matching, bandwidth enhancement, and antenna radiation characteristics improvement. The pi-shaped slot, which is a modified inverted U-shaped slot, is well-known for its relatively large impedance bandwidth. Hence, the dimensions of the pi-slot are adjusted to achieve the lowest possible input reflection coefficient of the antenna around the resonant frequencies, and their position is chosen so that the radiating structure can produce a wider bandwidth through multiple resonances while also providing proper impedance matching at the higher end of the operating range, ensuring stable performance across the full THz band.

III. RESULTS AND PARAMETRIC INVESTIGATION

The design, simulation, parametric investigation and performance analysis of the pi-shaped slotted patch antenna has been carried out high-performance EM solver CST-MWS. The performance of the proposed antenna has been investigated by computing S11, bandwidth, gain, directivity, efficiency, and radiation pattern, and surface current density from the simulator.

Fig. 2 demonstrates the impact of incorporating a pi-shaped slot on the elliptical patch of the proposed THz antenna design. It compares the reflection coefficient (S11) of the proposed antenna with and without a pi-slot. The antenna with the slot shows lower S11 values at key frequencies, indicating better impedance matching, reduced reflection, and improved performance. The inclusion of the pi-slot effectively reduces the return loss and alters the peak positions of the proposed antenna. The operating range of frequencies of the antenna is 5.01 to 8.42 THz. A minimum S11 of −43.57 dB is observed at 5.645 THz, indicating excellent impedance matching. The presence of two distinct resonant dips (at 5.645 and 7.715 THz) suggests the antenna is designed for multi-band THz operation, which is valuable for applications like THz imaging, spectroscopy, or high-speed wireless communication.

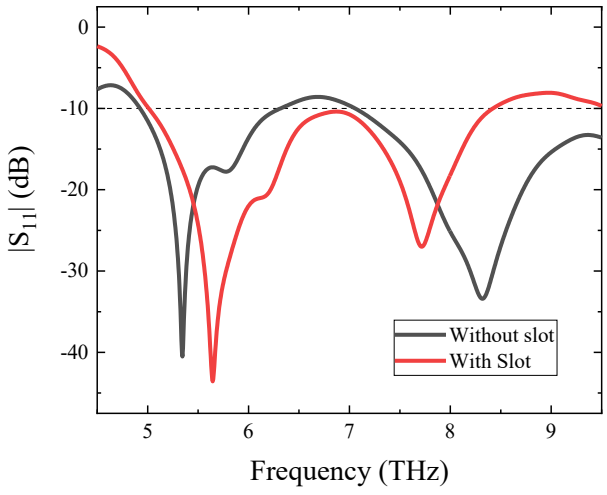

Fig. 2. Comparison of $|S_{11}|$ for proposed antenna with and without the pi-slot.

The reason behind the shifting of the resonant frequencies are as follows. The pi-slot elongates the path that surface currents follow, effectively increasing the electrical length of the antenna, and lowers the fundamental resonant frequency. The pi-slot introduces discontinuities that support multiple current loops, each capable of resonating at different frequencies. This leads to additional resonant peaks and broader bandwidth. The slot acts as a combination of inductive and capacitive elements. These reactive components shift the resonance by modifying the input impedance and phase response. The slot also alters the distribution of the electric and magnetic fields on the patch, which changes the boundary conditions and shifts the natural resonant modes. It can couple different parts of the patch or ground plane, introducing mutual coupling that shifts resonant frequencies.

The variation of S11 with different semi-major axis (Xr) of the presented THz antenna is shown in Fig. 3, which depicts that increasing the Xr while keeping the semi-minor axis (Yr) constant leads to a downward shift in both primary and secondary resonant frequencies. As Xr increases (40 to 49 µm), the resonance frequency shifts downward. Larger Xr values effectively increase the electrical length of the resonant structure, lowering the natural frequency. Xr = 40 µm (black) resonates at a higher frequency. Xr = 49 µm (blue) resonates at a noticeably lower frequency. The bandwidth broadens with increasing Xr. At smaller Xr (40 µm), the resonance dip is sharper and narrower. At larger Xr (46–49 µm), the dips are wider, meaning the device maintains good impedance matching across a broader frequency range. The resonance depth (minimum S_{11}) also improves slightly with larger Xr, indicating better matching. Xr = 49 µm shows both deep resonance and wide bandwidth, making it robust in terms of performance.

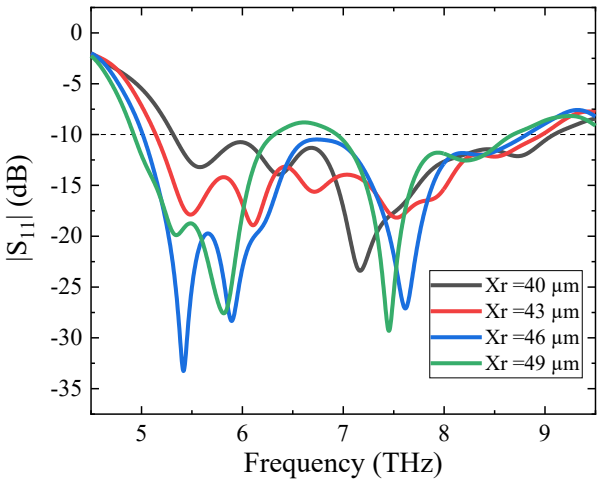

Fig. 3. Variation of |S11| with different Xr.

Fig. 4 shows the variation of radiation efficiency with different Xr of the proposed antenna. All curves show a sharp rise in efficiency from ~4 THz to ~5 THz, then stabilize. Efficiency improves consistently with increasing Xr, indicating better radiation characteristics. Increasing the Xr enhances the effective aperture and current distribution, reducing losses and improving radiation. Larger Xr values likely improve impedance matching and mode confinement, contributing to higher efficiency. Xr of 49 µm yields the best radiation efficiency across the 4–9 THz range. This makes it ideal for applications requiring power-efficient transmission, such as THz imaging, sensing, or communication.

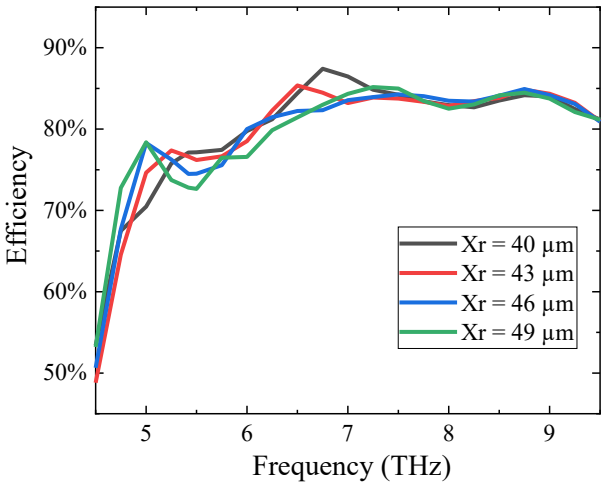

Fig. 4. Variation of efficiency with different Xr.

Fig. 5 shows the variation of gain with different Xr for the designed antenna. As seen from Fig. 5, the directional gain increases from 3.2 dB to 8.2 dB with increasing frequency for all designs with different Xr while keeping the Yr constant. At smaller Xr (40 µm), the gain peaks are slightly lower and occur at higher frequencies. As Xr increases, the gain peak values rise modestly, with Xr = 46 µm and 49 µm showing stronger gain performance across the mid-THz band.

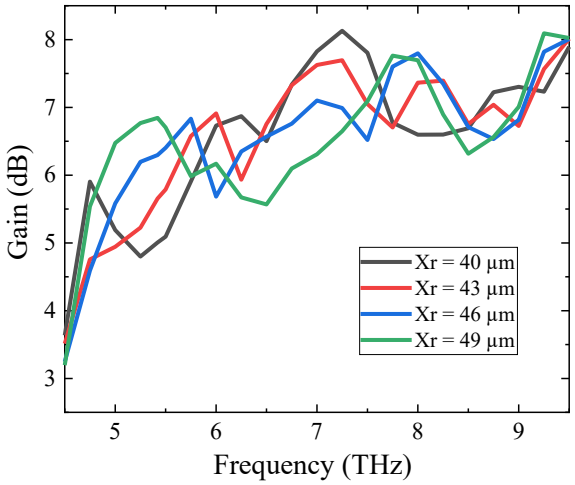

Fig. 5. Variation of gain with different Xr.

Fig. 6 depicts the variation of S_{11} with different length of feedline (Lf) of proposed THz antenna. It is evident from Fig. 6

that as Lf increases (22.04 to 32.04 µm), the resonant frequency shifts downward. A larger Lf increases the effective path length of the resonant structure, lowering its natural frequency. At smaller Lf (22.04 µm), the resonance dip is shallower (around –20 to –25 dB), indicating weaker matching. As Lf increases, the resonance depth improves, with Lf = 30.04 µm and 32.04 µm showing deeper dips (~ –35 to –40 dB), meaning stronger impedance matching and reduced reflection. The dips also broaden slightly with larger Lf, suggesting improved bandwidth. Smaller Lf values produce sharper, narrower resonances, while larger Lf values yield wider operational ranges.

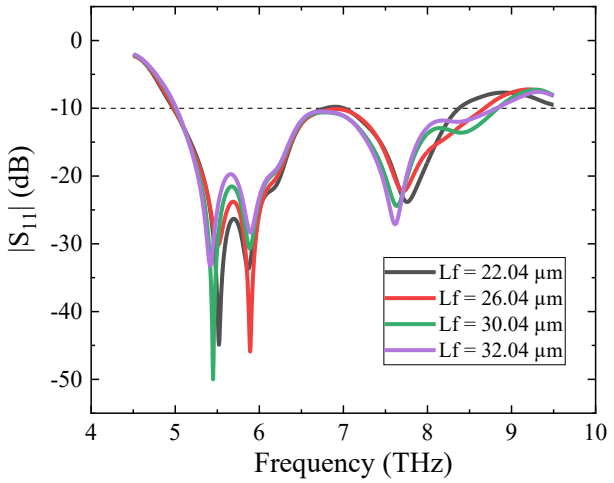

Fig. 6. Variation of |S11| with different Lf.

Fig. 7 illustrates how efficiency varies with frequency for different values of Lf across the THz band. As seen the efficiency varies from 55% to 85% in the operating THz range of frequencies. All curves show a rapid initial rise (4.5–5.5 THz) in efficiency, where larger Lf values (e.g., 30.04 µm, 32.04 µm) reach higher efficiency slightly earlier compared to smaller Lf values. Then it stabilizes across the band. There is a plateau region (5.5–9.5 THz) where efficiency stabilizes between ~75–85%. The higher Lf values sustain slightly higher efficiency across the plateau by enhancing impedance matching and mode coupling. For example, Lf = 32.04 µm (purple) maintains efficiency closer to the upper bound (~85%), while Lf = 22.04 µm (black) sits nearer the lower bound (~75–78%).

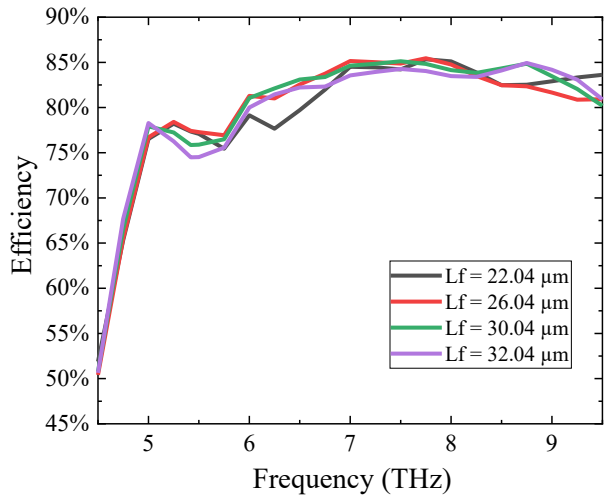

Fig. 7. Variation of efficiency with different Lf.

Fig. 8 illustrates how the parameter Lf influences gain across the THz frequency band. As Lf increases, the peak gain shifts toward lower frequencies. Smaller Lf values (22.04 µm) yield higher peak gain (~8.5–9 dB), while larger Lf values (32.04 µm) produce lower peak gain (~6–7 dB). Thus, increasing reduces the achievable peak gain at lower range of frequencies. At higher range of frequencies, at smaller Lf (22.04 µm), the gain peaks are lower (around 5–6 dB). As Lf increases, the gain peak values rise, with Lf = 30.04 µm and 32.04 µm reaching closer to 8 dB.

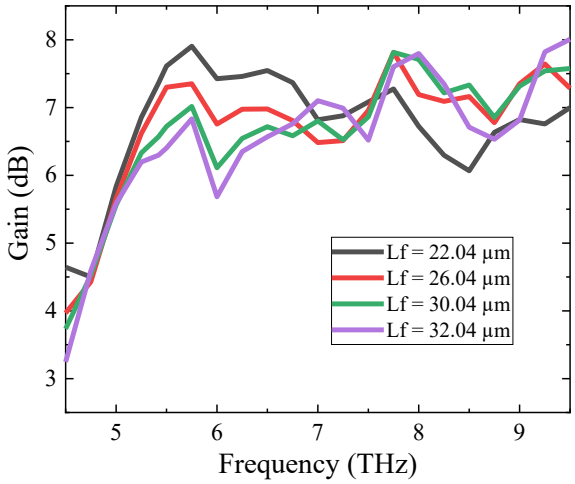

Fig. 8. Variation of gain with different Lf.

Fig. 9 depicts the influence of Top-End Width of Feedline (Fw1) on the antenna's reflection behavior. Narrower feedlines (8 µm) tend to resonate at lower frequencies due to higher inductance. Wider feedlines (14 µm) shift resonance upward but

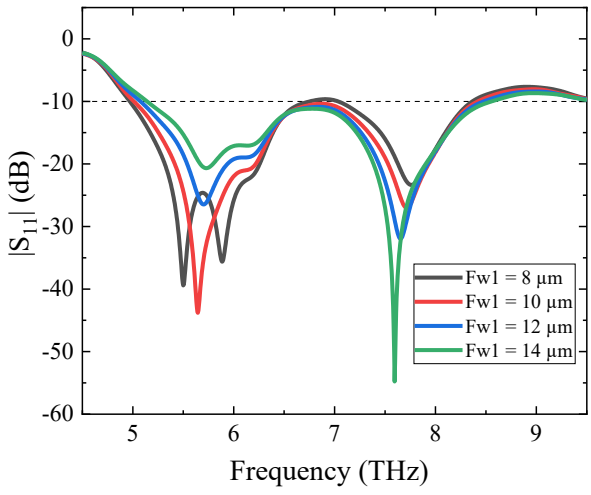

Fig. 9. Variation of S11 with different Fw1.

may degrade matching due to increased capacitive loading or altered current distribution. The 10 µm width feedline strikes the best balance, which offers broadband performance with multiple resonant dips.

Fig. 10 illustrates the impact of Fw1 on antenna's efficiency. All curves show a sharp increase in efficiency between 4.5 THz and 5 THz. Beyond 5 THz, efficiency stabilizes above 80% for all feedline widths. 8 µm shows slightly reduced performance, possibly due to higher conductor loss or impedance mismatch. 14 µm may introduce parasitic effects or altered current distribution, slightly degrading efficiency. The 10 µm wide feedline offers optimal radiation efficiency across the operating THz band.

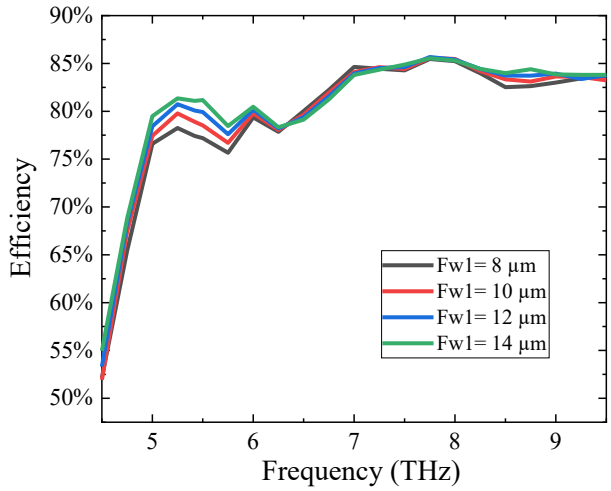

Fig. 10. Variation of efficiency with different Fw1.

Fig. 11 shows the impact of Fw1 on the THz antenna's gain. All curves show moderate gain variation across the band. Gain generally increases with frequency, peaking between 7 to 8 THz, then slightly tapering off. Smaller Fwl values yield higher peak gain at the resonant frequencies. In the operating range, the gain decreases from about 7.8 dB to about 6.2 dB, this is a reduction of roughly 1.6 dB across the range. So, a smaller Fwl value of 8 µm is chosen in the present design as a narrower feedline at the connection point to the patch ensures the transition from the 50 Ω feedline to the patch impedance is smooth, reducing mismatch and improving return loss and efficiency.

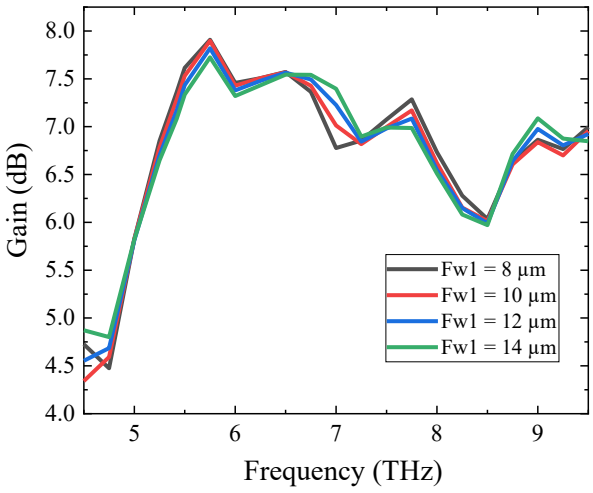

Fig. 11. Variation of gain with different Fw1.

The variation of S11 with frequency for different Pi slot length (A) of the presented THz antenna is shown in Fig. 12. The red curve for A=18 µm shows a strong dip well below -10 dB, indicating efficient impedance matching and reduced reflection. Around the resonant frequency, the -10 dB bandwidth for A = 18 µm is broader than for A = 16 µm or A = 22 µm. A = 16 µm gives a resonance but S11 not as deep as below -10 dB, while A = 20 µm and 22 µm shift the resonance but with less favorable reflection levels. The 18 µm case strikes the best balance between depth, bandwidth, and frequency positioning. Therefore, looking at the S11 plot, the case of A = 18 µm (red curve) appears better because it achieves a deeper and more stable resonant dip below the -10 dB threshold compared to the other values.

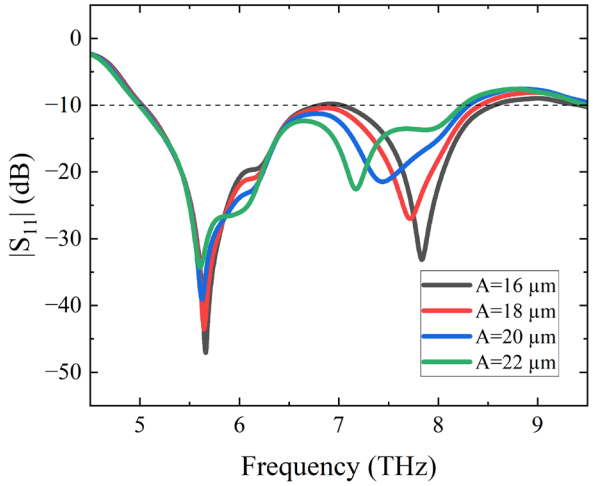

Fig. 12. Dependence of S11 on Pi slot length (A).

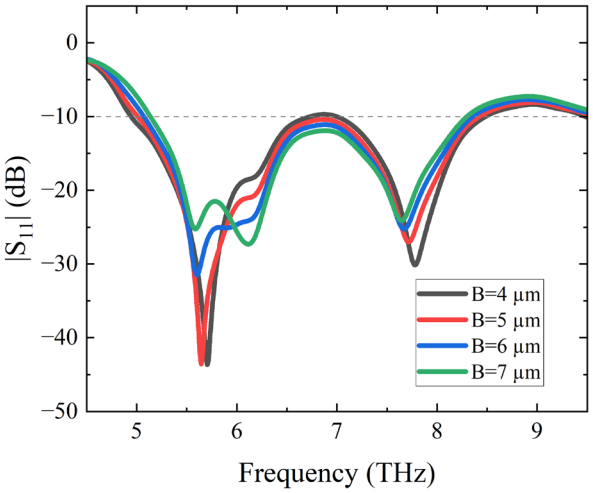

Fig. 13. Dependence of S11 on different width of pi slot (B).

Fig. 13 depicts the dependence of S11 versus frequency plot on different values of width of pi slot (B). As seen from the figure, the case of B = 5 µm (red curve) is better because it achieves a deeper and more effective resonance compared to the other values. B = 4 µm shows resonance but not as deep, while B = 6 µm and 7 µm shift resonance with weaker dips. The 5 µm case balances depth, bandwidth, and frequency positioning most effectively.

The dependence of S11 versus frequency plot on Legs length of pi slot (L) is shown in Fig. 14. As seen, L = 10 µm achieves a very deep resonance dip (close to –50 dB); the dip is relatively broad compared to L = 8 µm and 9 µm, meaning it covers a wider frequency range effectively. L = 11 µm also shows good bandwidth, but its resonance shifts lower in frequency. L = 11 µm is equally strong in matching but better suited if your design targets lower frequencies. When evaluating bandwidth and impedance matching (resonance depth) together, the best-performing case is L = 10 µm (blue curve).

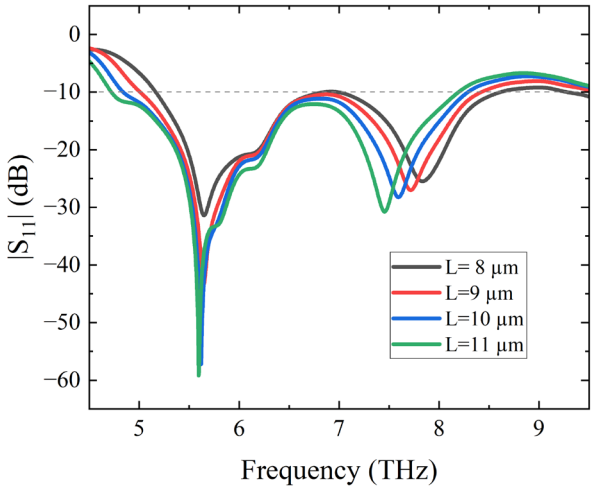

Fig. 14. Dependence of S11 on Legs length of pi slot (L).

Fig. 15 presents the simulated radiation efficiency of the proposed pi-shaped slotted elliptical patch antenna. The antenna possesses an efficiency of 77.43% at 5.645 THz, while exhibits ~70–85% efficiency within the operating range of 5.01 THz to 8.42 THz, confirming low loss and effective radiation. High radiation efficiency across the operating bands suggests the antenna is well-suited for THz applications requiring high power delivery, such as imaging, sensing, or high-data-rate communication.

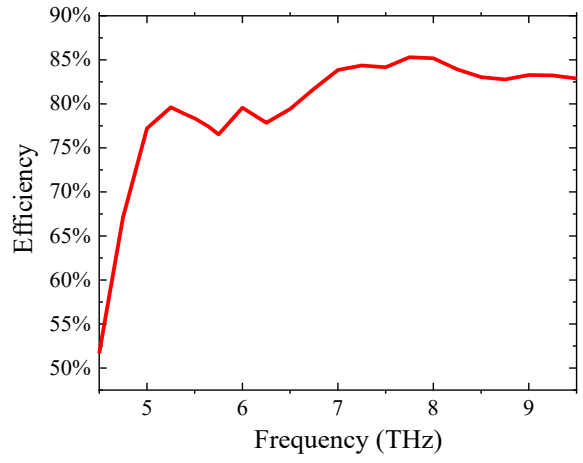

Fig. 15. Simulated radiation efficiency of the proposed antenna.

Fig. 16 presents the simulated VSWR (Voltage Standing Wave Ratio) of the proposed THz antenna over the frequency range 4.5 THz to 9.5 THz. A VSWR < 2 over a wide operating frequency band (5.01 to 8.42 THz) confirms the antenna achieves excellent impedance matching with efficient power transfer and minimal reflection losses, validating the antenna's suitability for broadband THz applications.

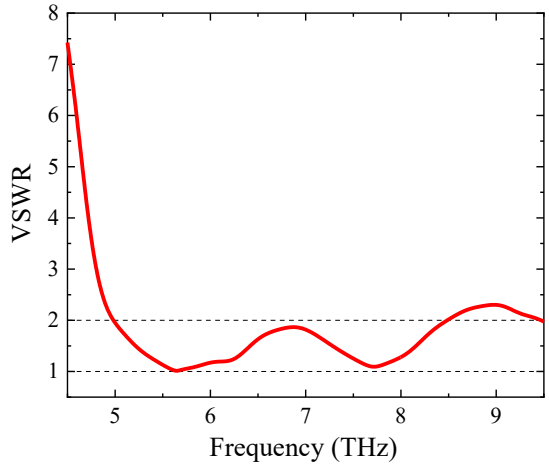

Fig. 16. VSWR of the proposed antenna.

Gain pattern of the pi-shaped slotted elliptical patch antenna at 5.645 THz is depicted in Fig. 17(a), while its directivity pattern is presented in Fig. 17(b). At 5.645 THz, the antenna exhibits a gain of 7.906 dB and a directivity of 9.017 dBi. Fig. 17(c) shows the gain and directivity performance of the proposed THz antenna over the range 4.5 to 9.5 THz. Gain peaks at ~5.6 THz, fluctuates 4.32 to 6.05 dB, and remains above 6 dB across most of the spectrum, supporting strong radiation. The antenna demonstrates consistently high directivity across the operating THz range, fluctuating between 6.0 dBi and 9.5 dBi, indicating strong directional radiation characteristics throughout the operating band. These results confirm its suitability in focused THz applications such as point-to-point communication, imaging, and sensing.

Gain fluctuations across the specified frequency band may stem from several interrelated physical and design factors like resonant mode behavior, slot geometry effects, Impedance mismatch, and surface current distribution. The present UWB antennas are designed to function across multiple resonant modes, thereby enabling enhanced performance over a broad frequency spectrum. Each mode may radiate differently, leading to peaks and dips in gain at various frequencies. The slot introduces multiple resonances. While this helps bandwidth, it can also cause uneven gain due to varying coupling strength at differ-

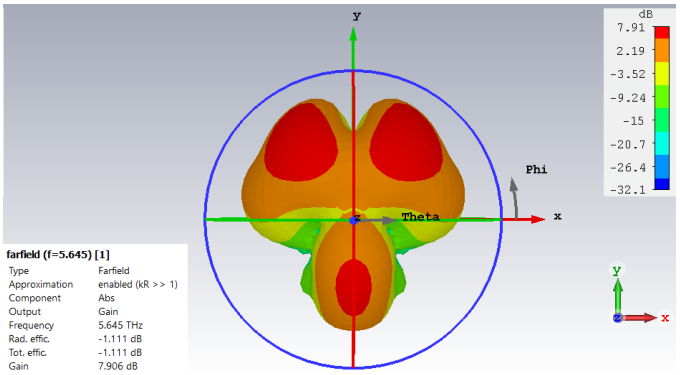

(a)

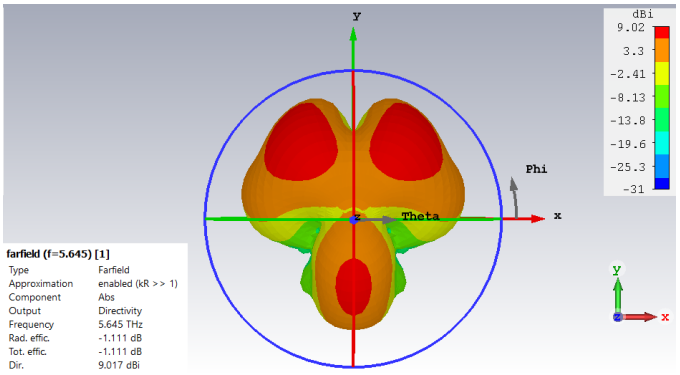

(b)

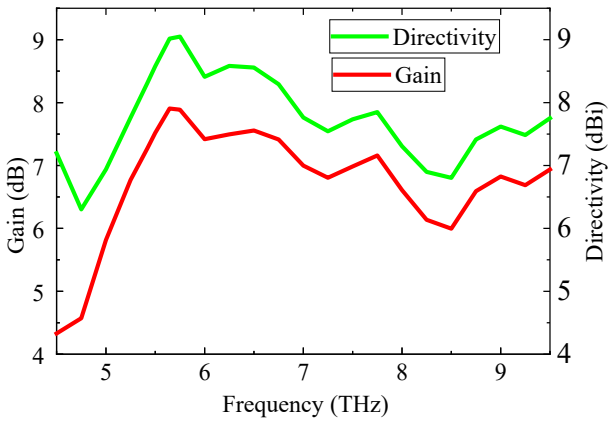

(c)

Fig. 17. (a) 3D farfield gain pattern, (b) 3D farfield directivity pattern, (c) Gain and directivity versus frequency for the proposed THz antenna over the operating frequency range.

ent frequencies. Even with good return loss, perfect impedance matching across the entire UWB band is difficult. Minor mismatches at certain frequencies can reduce radiation efficiency, causing gain dips. The current paths on the patch and ground plane change with frequency. At higher frequencies, these paths may become less efficient or radiate in undesired directions.

Fig. 18 presents the polar plot of the far-field electric field (E-field) and magnetic field (H-field) at a frequency of 5.645 THz for φ = 0º and 90º. At φ = (0°, 90°), the main lobes of the E-field and H-field patterns are focused at (0°, 29°), with respective magnitudes of (15.1 dB V/m, 20.8 dB V/m) and (−36.4 dBA/m, −30.7 dBA/m). The 3 dB angular beamwidths are (47.7°, 21.3°), and the side lobe level is −2 dB. The narrow beamwidth and low side lobe level imply a highly directional antenna, ideal for THz applications requiring spatial precision such as targeted sensing, imaging, or line-of-sight communication where spatial resolution and minimal interference are critical.

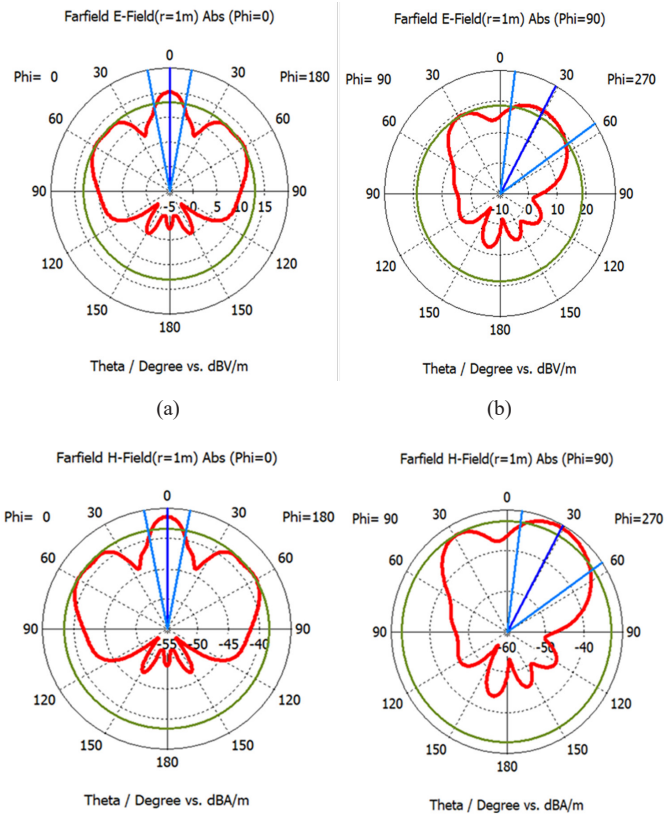

(a) (b) (c) (d)

Fig. 18. 2D Farfield E-Field pattern at 5.645 THz for (a) Ø=0°, (b) Ø=90° and H-field pattern for (c) Ø=0°, (d) Ø=90°.

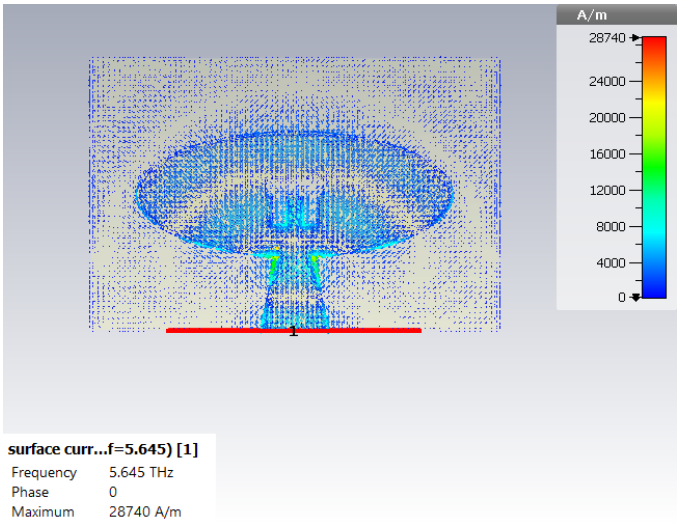

Fig. 19. Surface current at 5.645 THz.

Fig. 19 shows the simulation result of the surface current distribution of the proposed antenna at 5.645 THz. The maximum surface current density of 28,740 A/m occurs at the lower part of the feedline, the lower edges of the patch, and the slot, attributed to field enhancement and boundary conditions.

Table II shows a summary of the performance metrics of the proposed THz antenna. The low VSWR and high return loss confirm that the antenna is well-tuned to its operating frequency. The wide bandwidth and compact size make it suitable for on-chip THz communication, spectroscopy, or imaging systems. This antenna demonstrates excellent impedance matching, high gain, directivity, and efficiency at terahertz frequencies. Input impedance is very close to the standard 50 Ω, which ensures its compatibility with THz transmission lines and measurement equipment. It balances compact size, broad bandwidth, and high efficiency, which is rare at such high frequencies. The present compact THz antenna achieves a notable gain of 7.906 dB, underscoring its effectiveness for directional transmission and reception in point-to-point THz communication systems. High directivity (9.017 dBi) indicates focused radiation, which is ideal for targeted sensing or communication. Max Surface Current of 28,740 A/m indicates strong resonance and active current regions.

Table II
Performance of the Proposed THz Antenna

Size	120×80 (9600 μm²)
Return loss	-43.57 dB (at 5.645 THz)
Bandwidth	3.41 THz
VSWR	1.01 (at 5.645 THz)
Radiation efficiency	77.43% (at 5.645 THz)
Gain	7.906 dB (at 5.645 THz)
Directivity	9.017 dBi (at 5.645 THz)
Impedance	50.704 Ω (at 5.645 THz)
Surface current	28740 A/m (at 5.645 THz)

IV. Comparative analysis

Table III presents a comparative analysis of the proposed antenna's strengths and compatibility with previous designs. The proposed pi-slotted elliptical patch antenna achieves a maximum bandwidth of 3100 GHz within a compact footprint of 120 × 80 μm² (9600 μm²), and demonstrates excellent radiation characteristics including VSWR of 1.01, reflection coefficient of −43.57 dB, gain of 7.906 dB, and efficiency of 77.43%.

The present design has the smallest footprint (9,600 μm²), ideal for integration in THz chips or compact modules. [7] offers excellent performance but at 1,000,000 μm², which is impractical for miniaturized systems. [7] leads with -64.16 dB, indicating super impedance matching. *This Work* and [22] both show -43.57 dB, which is still excellent and highly efficient for THz operation. "This Work" achieves the widest bandwidth: 0.5–4.82 THz (≈3100 GHz), supporting ultra-broadband THz applications. [22] follows with 2.72–4.52 THz (≈1250 GHz), still impressive but narrower. "This Work" reach 7.906 dB, the highest among all entries, ensuring strong signal transmission.

Ref. [7] tops with 98% efficiency, but again, its size is a limiting factor. "This Work" maintains a solid 77.43% efficiency, balancing compactness with respectable efficiency. Elliptical patch designs ([22], "This Work") outperform others in gain and bandwidth, likely due to smoother current distribution and broader resonant modes. Rectangular and hybrid shapes [8], [9], [19], show moderate performance, often limited by narrower bandwidth and lower gain.

Proposed antenna design stands out as the most balanced and optimized THz solution, offering: Ultra-compact size, Exceptional bandwidth, High gain, and Strong efficiency. It is particularly well-suited for next-generation THz systems requiring miniaturization, broadband capability, and high-performance radiation. In THz systems, miniaturization, broadband capability, and high radiation efficiency are critical. "This Work" achieves an optimal balance of these factors, making it a strong candidate for: On-chip THz communication, High-resolution imaging, and Spectroscopy and sensing applications.

Table III
Comparison with Existing THz Antennas

Ref. No.	Antenna Size (μm2) ($\lambda_g \times \lambda_g$)	Patch Shape/ Substrate	S11 (dB)	Bandwidth (GHz)	Gain (dB)	Efficiency (%)
[7]	1000 × 1000 ($12.33\lambda_g \times 12.33\lambda_g$)	Square/ Polyimide	-64.16	26.7 (2.15–2.2 and 2.56–2.6 THz)	6.793	98
[8]	208 × 180 ($1.216\lambda_g \times 1.052\lambda_g$)	Rectangular/ Silicon	−21.67	50 (0.696 THz)	4.01	64.12
[9]	100 × 100 ($4.81\lambda_g \times 4.81\lambda_g$)	Rectangular & Circular/ Si and Teflon	−57.54	199.6 (5.5 THz)	2.76	–
[10]	24 × 24 ($0.30\lambda_g \times 0.30\lambda_g$)	Square loop / Polyimide	−28	38 (2.3 THz)	5	60
[18]	300 × 300 ($0.852\lambda_g \times 0.852\lambda_g$)	Circular ring / Polyimide	−24.5	415 (0.523–0.9395 THz)	5.87	80
[19]	500 × 500 ($2.68\lambda_g \times 2.68\lambda_g$)	Rectangular/ FR4	−16.86	92 (0.761 -0.853 THz)	6.14	–
[22]	140 × 100 ($1.43\lambda_g \times 1.02\lambda_g$)	Elliptical/ Rogers	−27.08	1250 (2.12-3.37 THz)	7.769	89
This Work	120×80 ($2.83\lambda_g \times 1.89\lambda_g$)	Elliptical/ Rogers	-43.57	3100 (5.01-8.42 THz)	7.906	77.43

V. Conclusions

In the THz frequency domain, the development of microstrip patch antennas capable of supporting high data rates and wide bandwidth poses a significant engineering challenge. This paper proposes a compact UWB elliptical patch antenna featuring a pi-shaped slot and a 50 Ω tapered feedline to address the demand for high data rate THz transmission. An elliptical patch antenna has been designed with a pi-shaped slot for the first time in the THz spectral region, enabling simultaneous size miniaturization, wideband or multi-band performance, improved impedance matching, and enhanced gain. Optimizing the dimensions and geometry of the patch, slot, and feedline was crucial for achieving wide bandwidth and low return loss. The antenna size is compact 120×80×6 μm3. The simulation result obtained from CST simulator has shown the proposed antenna exhibited broad impedance bandwidth of 3.41THz (from 5.01 to 8.42 THz), high gain of 7.906 dB, high directivity of 9.017 dBi acceptable radiation efficiency of 77.83%, and low return loss of -43.57 dB and low VSWR 1.0, surface current of 28740 A/m at 5.645 THz. The proposed antenna supports ultra-high data rates owing to its wide bandwidth of 3.41 THz. Additionally, it achieves a gain of 7.906 dB and an efficiency of 77.83%. With its simple feeder structure, low manufacturing cost, wide bandwidth, and high gain, the proposed antenna presents a suitable candidate for THz high-speed communication applications. In future work, Machine learning algorithms can be applied to optimize antenna geometries, predict performance, and accelerate prototyping. The antenna's performance can be improved by applying different performance enhancement methods and with the use of advanced materials and metamaterials.

Future work will focus on developing suitable measurement setups to experimentally validate the radiation characteristics and further strengthen the reliability of the proposed design. Simulation will be performed for the same design with the TLM mesh using the CST. Future works will also aim to develop a theoretical model to the design process of the Pi slotted THz antenna. The skin effect and surface roughness will also be accounted in the simulations.

References

[1] I. F. Akyildiz, J. M. Jornet, and C. Han, "Terahertz band: Next frontier for wireless communications," *Physical Communication*, vol.12, pp. 16-32, 2014, DOI: 10.1016/j.phycom.2014.01.006.

[2] A. N. Bharadwaj, A. M. Kashyap, G. B. N, R. Jayachandran and R. Kishore, "A Survey on Terahertz Devices-A cutting edge Technology," in Proc. *2023 Int. Conf. on Recent Trends in Electronics and Communication (ICRTEC)*, Mysore, India, pp. 1-6, DOI: 10.1109/ICRTEC56977.2023.10111851.

[3] S. Elaage, M. El Ghzaoui, N. Mrani, R. El Alami, A. El Alami, M. O. Jamil, and H. Qjidaa, "Modeling and analysis of short distance terahertz communication channel," in *Lecture Notes in Networks and Systems (LNNS)*, vol. 669, pp 289–297, 2023, DOI: 10.1007/978-3-031-29860-8_30.

[4] I. Akyildiz, J. Jornet, and C. Han, "TeraNets: Ultra-broadband communication networks in the terahertz band," *IEEE Wireless Commun.*, vol. 21, no. 4, pp. 130–135, Aug. 2014, DOI: 10.1109/MWC.2014.6882305.

[5] Z. Jin, Y. Rong, J. Yu, and F. Wu, "Design of a compound reconfigurable terahertz antenna based on graphene," *Plasmonics*, vol. 19, pp. 621–629, 2024. DOI: 10.1007/s11468-023-02011-8.

[6] R. Pant, and L. Malviya, "THz antennas design, developments, challenges, and applications: A review," *International Journal of Communication Systems*, Vol. 36, Issue 8, e5474, 2023, DOI: 10.1002/dac.5474.

[7] S. Mrunalini, and A. Manoharan, "Dual-band re-configurable graphene-based patch antenna in terahertz band for wireless network-on-chip applications," *IET Microwaves, Antennas & Propagation*, vol. 11, pp.2104-08, 2017, DOI: 10.1049/iet-map.2017.0415.

[8] S. Ullah, C. Ruan, T. U. Haq, and X. Zhang, "High performance THz patch antenna using photonic band gap and defected ground structure," *Journal of Electromagnetic Waves and Applications*, vol. 33, pp. 1943-54, 2019, DOI: 10.1080/09205071.2019.1654929.

[9] M. A. Khan, T. A. Shaem, and M. A. Alim, "Analysis of graphene based miniaturized terahertz patch antennas for single band and dual band operation," *Optik*. Vol. 194, pp.163012, 2019, DOI: 10.1016/j.ijleo.2019.163012.

[10] K. Vijayalakshmi, C. K. Selvi, and B. Sapna, "Novel tri-band series fed microstrip antenna array for THz MIMO communications," *Optical and Quantum Electronics*, vol. 53, pp. 395, 2021, DOI: 10.1007/s11082-021-03065-w.

[11] B. Moulfi, S. Ferouani, D. Ziani-Kerarti, and W. Moulessehoul, "Wide Band Nano Circular Graphene Printed Antenna for Terahertz Transmission with DGs," *Telecommunications and Radio Engineering,* vol. 81, pp. 37 2022, DOI: 10.1615/TelecomRadEng.2022042936.

[12] M. A. K. Khan, T. A. Shaem, and M. A. Alim, "Graphene patch antennas with different substrate shapes and materials," *Optik*, vol. 202, pp. 163700 2020, DOI: 10.1016/j.ijleo.2019.163700.

[13] A. Abohmra, F. Jilani, H. Abbas, M. A. Imran and Q. H. Abbasi, "Terahertz Antenna based on Graphene for Wearable Applications," in *2019 IEEE MTT-S International Wireless Symposium (IWS)*, Guangzhou, China, pp. 1-3, DOI: 10.1109/IEEE-IWS.2019.8803929.

[14] M. M. Fakharian, "A graphene-based multi-functional terahertz antenna," *Optik*, vol. 251, pp. 168431, 2022, DOI: 10.1016/ j.ijleo.2021.168431.

[15] N. S. Badr, and G. Moradi, "Graphene-Based microstripfed hexagonal shape dual band antenna," *Optik*, vol. 202, pp. 163608, 2020, DOI: 10.1016/j.ijleo.2019.163608.

[16] G. Nissiyah, and M. Ganesh, "Analysis of single band and dual band graphene based patch antenna for terahertz region," *Physica E: low-dimensionl systems and nanostructures*, vol. 94, pp. 126131, 2017, DOI: 10.1016/j.physe.2017.08.001.

[17] P.-L. Sun, "420-GHz terahertz SIW slot antenna with quartz superstrates in silicon technology," *Optoelectron. Lett.,* vol. 16, pp. 25–28, 2020, DOI: 10.1007/s11801-020-9063-8.

[18] W. A. Khan, and A. B. Muhammad, "Design and analysis of wideband THz micro size patch antenna for 6G application," in *Proc. 6th IEEE Int. Conf. on Millimeter-Wave and Terahertz Technologies (MMWaTT)*, Tehran, Iran, pp.1-4, 2022, DOI: 10.1109/MMWaTT58022.2022.10172086.

[19] K. K. Naik, "Asymmetric CPW-fed patch antenna with slits at terahertz applications for 6G wireless communications," *Wireless Networks*, vol. 30, pp. 2343-51, 2024, DOI: 10.1007/s11276-024-03695-4.

[20] D. M. Pozar, *Microwave Engineering*, Wiley, Hoboken, NJ, USA, 2011, pp. 115-135, ISBN: 978-0470631553.

[21] R. Garg, P. Bhartia, I. Bahl, and A. Ittipiboon, *Microstrip Antenna Design Handbook*, Artech House, Norwood, MA, USA, 2001, pp. 15-42, ISBN: 978-0890065136.

[22] R. Masum, M. Islam, S. Roy, M. F. Ahmed, M. M. Islam, M. R. Hossain, and R. Sarkar, "A Slotted Elliptical Patch Antenna for Six Generation Communication System in Terahertz Band," *Cureus J Eng* 2, es44388-024-02717-3, January 25, 2025, DOI: 10.7759/s44388-024-02717-3.